Enhanced antibacterial performance of ultrathin silver/platinum nanopatches by a sacrificial anode mechanism

Adham Abuayyash, MSc[a], Nadine Ziegler, MSc[b], Hajo Meyer, PhD[b], Michael Meischein, MSc[b], Christina Sengstock, PhD[a], Julian Moellenhoff, Cand Med[a], Christian Rurainsky, MSc[c], Marc Heggen, PhD[d], Alba Garzón-Manjón, PhD[e], Christina Scheu, PhD[e], Kristina Tschulik, PhD[c], Alfred Ludwig, PhD[b], and Manfred Köller, PhD,[a,]*

[a] *BG University Hospital Bergmannsheil, Surgical Research, Buerkle-de-la-Camp-Platz 1, 44789 Bochum, Germany*

[b] *Ruhr University Bochum, Institute for Materials, Faculty of Mechanical Engineering, Universitätsstraße 150, 44801 Bochum, Germany.*

[c] *Ruhr University Bochum, Faculty for Chemistry and Biochemistry, Analytical Chemistry II, Universitätsstraße 150, 44801 Bochum, Germany.*

[d] *Forschungszentrum Jülich, Ernst Ruska-Center for Microscopy and Spectroscopy with Electrons, Wilhelm-Johnen-Straße, 52428 Jülich, Germany.*

[e] *Max-Planck-Institut für Eisenforschung GmbH, Max-Planck-Straße 1, 40237 Düsseldorf, Germany.*

* corresponding author, Manfred.Koeller@rub.de

Word count for abstract: 149
Word count for manuscript: 4120
Number of references: 31
Number of figures: 7
Number of tables: 0
Number of Supplementary online-only files, if any: 1

This work was supported by the Deutsche Forschungsgemeinschaft (DFG) KO 1302/8-1 and LU 1175/21-1. K.T. was supported by the Ministry of Innovation, Science and Research of North Rhine-Westphalia (NRW Rückkehrerprogramm). We thank Mr. Samuel Müller-Späth for his contributions to this work during his master thesis.

Conflict of Interest: All authors declare no conflict of interest.

Abstract

The development of antibacterial implant surfaces is a challenging task in biomaterial research. We fabricated a highly antibacterial bimetallic platinum (Pt)/silver(Ag) nanopatch surface by short time sputtering of Pt and Ag on titanium. The sputter process led to a patch-like distribution with crystalline areas in the nanometer-size range (1.3 - 3.9 nm thickness, 3-60 nm extension). Structural analyses of Pt/Ag samples showed Ag- and Pt-rich areas containing nanoparticle-like Pt deposits of 1-2 nm. The adhesion and proliferation properties of S.aureus on the nanopatch samples were analyzed. Consecutively sputtered Ag/Pt nanopatches (Pt followed by Ag) induced enhanced antimicrobial activity compared to co-sputtered Pt/Ag samples or pure Ag patches of similar Ag amounts. The underlying sacrificial anode mechanism was proved by linear sweep voltammetry. The advantages of this nanopatch coating are the enhanced antimicrobial activity despite a reduced total amount of Ag/Pt and a self-limited effect due the rapid Ag dissolution.

Background

The development of biomaterials with antibacterial surfaces which hinder or prevent bacterial adhesion and colonization of an implant surface is a challenging task in biomaterial research. Due to the increasing emergence of antibiotic resistant pathogens and accompanying serious clinical consequences several strategies apart from antibiotics have been developed which should inhibit initial bacterial colonization, either by surface topography or by special coatings.[1-3]

Among various coatings, silver (Ag) regained a standing due to its broad antibacterial activity (both gram-negative and positive bacteria) and a low incidence to induce bacterial resistance.[3, 4] The antibacterial activity of Ag is initiated by an oxidative dissolution which leads to the release of Ag ions (Ag+).[5, 6] This release of Ag+ represents the onset of the antibacterial effects, however, further Ag species such as AgCl or Ag-organic complexes are subsequently formed by metabolism.[7, 8] It is likely that these compounds are involved in biological effects of Ag but their antibacterial activities are less understood.[9-11] Nevertheless, any increase in

Ag+ release from an Ag surface will consequently lead to an increase in antibacterial activity Due to the large surface to volume ratio Ag nanoparticles (nanosilver) have gained attraction during the last decades and led to numerous reports (cf. recent reviews).[6, 12] However, the applications of nanosilver are still controversial and exposure to nanosilver may induce additional risks for medical application such as unwanted tissue reactions.[13, 14] In addition, the nanoscale particles have to be embedded into a coating on an implant surface or otherwise fixed onto the implant.

Recently, we presented an alternative mechanism to enhance Ag+ release by the use of the sacrificial anode principle.[15, 16] In contrast to technical applications (e.g. corrosion prevention) the sacrificial anode principle is hardly utilized for medical applications up to now. The sacrificial anode effect is based on an electrochemical mechanism. If two electrochemically different metals (or alloys) exist in an electrolytic environment, the less noble metal protects the more noble one by corroding, it is "sacrificed" in favor of the more noble part.[17] To develop a setup where Ag serves as the sacrificial anode it has to be combined with a more noble metal. In the past we demonstrated the feasibility of Ag sacrificial anode systems using microscale Ag dot arrays which were deposited on Au, Pd, Pt, or Ir thin films.[15, 16] These sacrificial anode dot arrays exerted a much higher antibacterial efficiency compared to same Ag dots on Ti (non-sacrificial anode for Ag) or to dense Ag thin films.[15, 16, 18]

There are good reasons to downsize the microscale sacrificial anode design to the nanoscale. Unlike the antibacterial mechanism of conventional antibiotics Ag toxicity is not selective for microorganisms. We have shown that the antibacterial effects of Ag nanoparticles occurred in the same concentration range as tissue cell toxicity.[19] Thus, any Ag release from an implant should be effective but a time-limited Ag ion release might be desirable to avoid accumulation of Ag within the adjacent tissue. A sacrificial anode system for Ag offers a downsizing approach by an enhanced Ag+ release at a low amount of needed Ag and may be highly effective for a limited time period. The reason is an electrochemically driven Ag+ release which can be significantly higher compared to Ag+ dissolution from a same size pure Ag surface.[15, 20]

Thus, it was the purpose of this study to generate nanosized Ag deposits (nanopatches) on a Ti surface which are in contact to similar Pt nanopatches to obtain a sacrificial anode system and to analyze structure and antibacterial efficiency of these nanopatches using material science, electrochemical, and microbiological methods.

Methods

Magnetron sputtering

The Ag-Pt nanopatches were fabricated via magnetron sputtering on Ti thin films or TEM grids using an AJA ATC-2200V sputter system. Three kinds of nanopatches were deposited for 20 s and 60 s: nanopatches which consists of pure Ag or pure Pt (reference samples), nanopatches with Pt first and then Ag on top, and nanopatches with both elements sputtered simultaneously (more details in supplementary materials).

Structural analysis

Structural analysis of nanopatches on TEM grids was performed by transmission electron microscopy (TEM) and scanning transmission electron microscopy (STEM). Compositional maps of nanopatches were obtained with energy-dispersive X-ray spectroscopy (EDX) (more details in supplementary materials).

Antibacterial activity

Bacterial tests were performed with *Staphylococcus aureus*. Bacteria were grown in BHI broth (brain-heart infusion broth. The adhesion and proliferation of the bacteria on the nanopatch samples were analyzed using a drop-based experimental setup (more details in supplementary materials).

Immersion in biological fluid

Partly samples were immersed in biological fluid. Therefore, nanopatch samples or nanopatches sputtered on TEM grids were deposited in 3 ml RPMI cell culture medium containing 10% fetal calf serum (FCS) and left in a cell culture incubator for 6 h or 3 days. Subsequently the samples were washed with A.dest., cultured with MSC or directly analyzed by TEM.

Linear sweep voltammetry

Electrochemical experiments were performed by linear sweep voltammetry in 1.0 M HCl (more details in supplementary materials).

Biocompatibility

Biocompatibility was analyzed using human mesenchymal stem cells (MSC). The adhesion and viability of the cells on the nanopatch samples were analyzed using a drop-based experimental setup (more details in supplementary materials).

Statistics

Quantification of antibacterial effects was performed by one-way ANOVA with Bonferroni post hoc test. p-Values < 0.05 were considered as statistically significant.

Results

The TEM images in Figure 1(A-C) show the shape and distribution of the sputter deposits (exemplarily for Ag) in dependence of growth time. The areas of the Ag islands, given as percentage of the total image area, were calculated as 15% (10 s), 19 % (20 s), and 33% (60 s). We assume, that the formation of those nanopatches is caused by the Volmer-Weber growth mechanism which predicts the formation of patches in the nanometer range instead of a continuous thin film.

The TEM characterization is shown for the nanopatches on the TEM grids whereas the Si/SiO_2 samples with the Ti thin film and nanopatches on top were used for the antibacterial tests. It was not possible to characterize the nanopatches on the Ti thin film with AFM or SEM due to the small size of the nanopatches and the roughness of the Ti thin film. Thus, the thickness of the nanopatches was calculated using the sputter rate which resulted in a nominal thin film thickness of 2.8 nm for 60 s.

Microstructural investigation of the Pt/Ag nanopatches (Pt20sAg20s consecutively sputtered sample) was performed using high angle annular dark field (HAADF) scanning transmission electron microscopy (STEM) and energy-dispersive X-ray spectroscopy (EDX) mapping. The HAADF-STEM image shows an irregular patch-like distribution with crystalline areas in the nanometer-size range (Figure 1 D). EDX investigation yields a local composition of Pt: 43 at% and Ag: 57 at% and demonstrates an irregular distribution of Ag- and Pt-rich areas

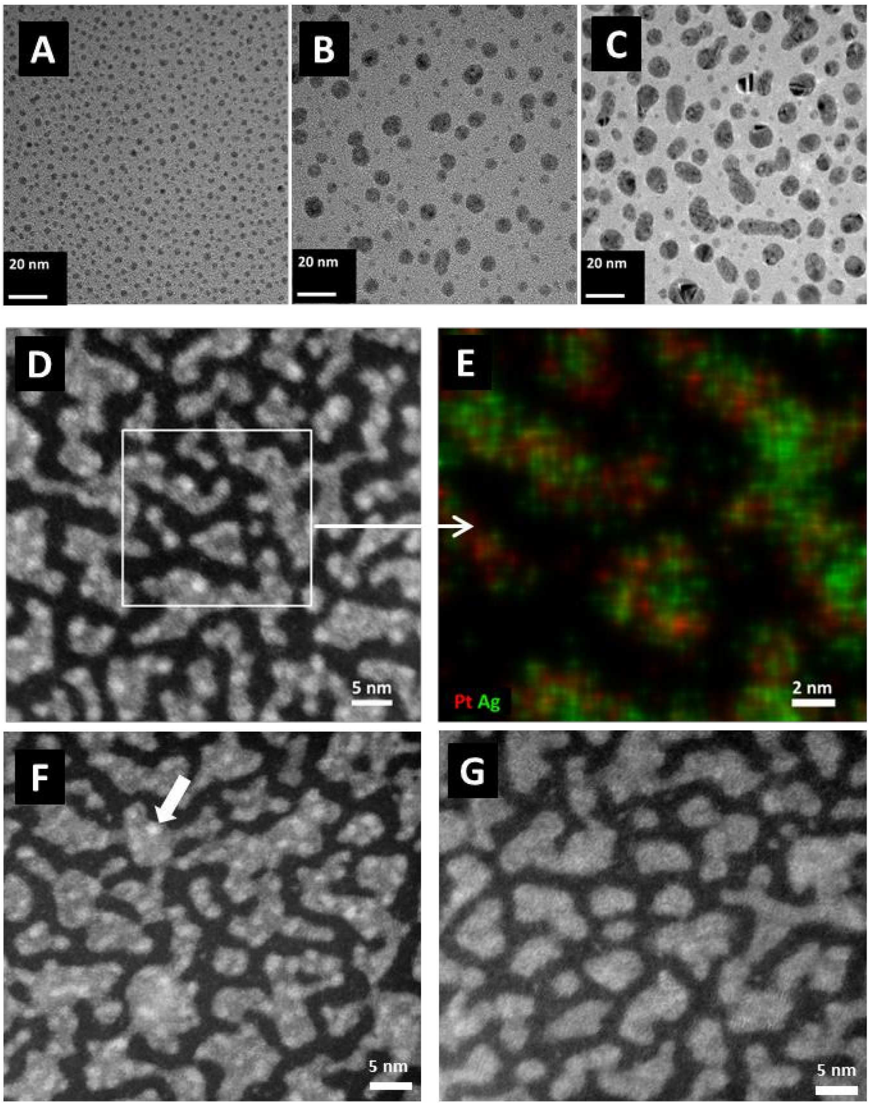

Figure 1. Microstructural analysis of sputter-deposited nanopatches. **A, B, C**: TEM analysis of sputtered Ag nanopatches (sputter times were A 10 s, B 20 s, C 60 s). **D**: HAADF-STEM image and **E**, the corresponding EDX map of the boxed region of consecutively sputtered Pt/Ag nanopatches (20 s) demonstrating an irregular distribution Pt (red) and Ag (green). **F**: consecutively sputtered Pt/Ag nanopatches (20 s, white arrow indicates Pt-rich spherical nanoparticle-like area). **G**: co-sputtered Pt/Ag nanopatches (20 s) with a more homogeneous elemental distribution.

(Figure 1 E). According to the Z-contrast conditions in HAADF-STEM imaging, local Pt-rich spherical nanoparticle-like areas with an average diameter of 1.2 nm are identified by a bright image contrast in the HAADF-STEM image and by direct comparison with the EDX map, whereas Ag-rich areas show a darker image contrast (Figure 1 D, F). The HAADF-STEM image of the co-sputtered sample (Figure 1 G) shows a more even contrast distribution compared to that of the consecutively sputtered sample (Figure 1 F). Therefore, a more homogeneous elemental distribution indicating a possible alloy-like structure is observed in the co-sputtered sample. The EDX quantification yields a composition of Pt: 38 at.% and Ag: 62 at%.

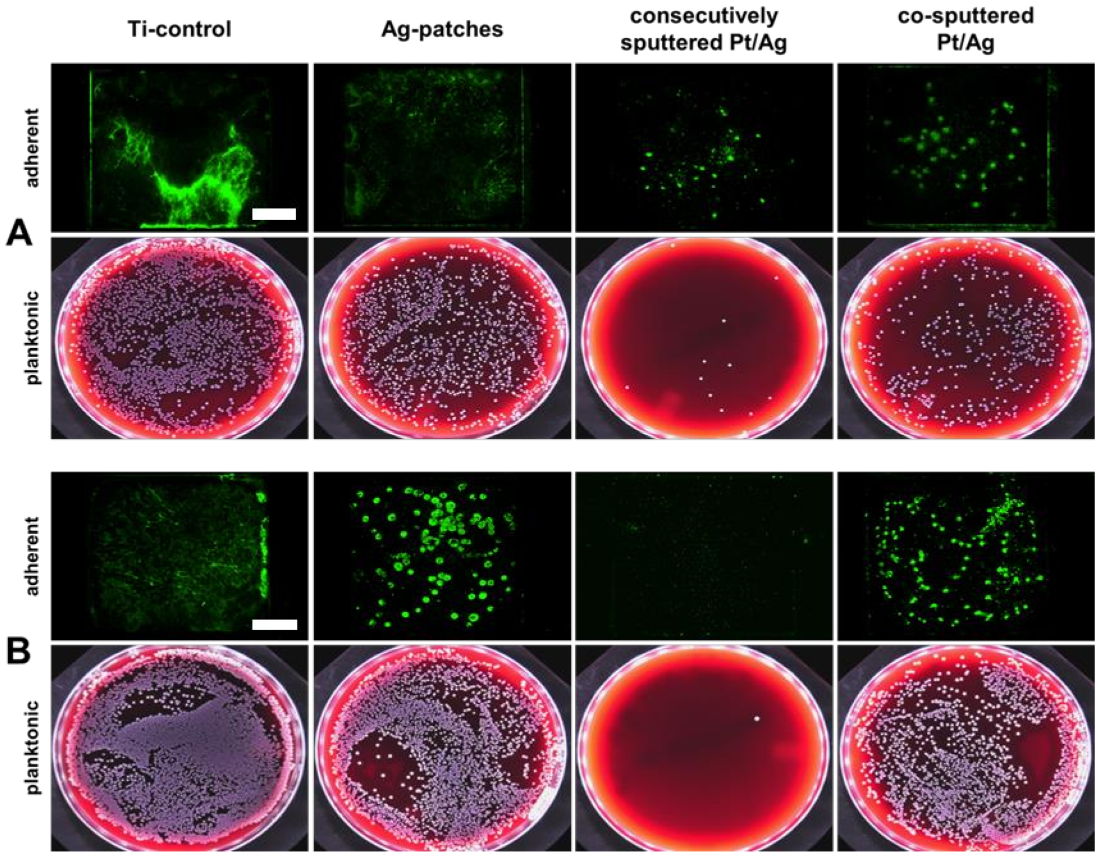

Figure 2. Antibacterial activity towards *S.aureus* of Ag nanopatches sputtered on Ti thin film compared to Ag/Pt nanopatches which were sputtered consecutively (first Pt, second Ag) or simultaneously (co-sputtered). Ti thin film without Ag patches serves as control (Ti control). **A**, samples generated with 20 s sputter time; **B** samples generated with 60 s sputter time. Upper figures: fluorescence images of adherent bacteria on the sample surfaces (whole sample); lower images: blood agar plates (8.5 cm diameter) which quantitatively demonstrate viable planktonic bacteria in the drop fluid as white bacterial colonies. Scale bars, 1 mm.

The antibacterial activity of nanoscale sacrificial anode samples (20 s and 60 s, both consecutively sputtered or co-sputtered) was analyzed toward *S.aureus* using a drop-based assay which allows the measurement of adherent and planktonic bacteria.[15, 16] Drops of bacteria within bacterial growth medium were placed onto the sample surfaces and were cultivated overnight. Subsequently, adherent bacteria were visualized by fluorescence microscopy. The planktonic bacteria within the drop fluid were quantified by conventional plating on blood agar after serial dilution of the aspirated drops. As is exemplarily shown in Figure 2 both 20 s (A) and 60 s (B) Pt/Ag nanopatches (consecutively sputtered and co-sputtered) exerted a higher antimicrobial activity compared to the Ag nanopatches of same Ag amount. This clearly demonstrated the sacrificial anode effect. Samples of pure Pt patches did not show any antibacterial effect (data not shown), correlating to our previous results on pure Pt thin films.[16]

Among the Pt/Ag nanopatches the consecutively sputtered samples significantly exerted the most efficient antibacterial activity (i.e. reduction in bacterial colonies) compared to same Ag patches alone (Ag patches) and co-sputtered (Pt-Ag patches). The statistical quantification of the obtained results is given in Figure 3. As is clearly shown, the consecutively sputtered Pt/Ag samples are significantly superior in the reduction of bacterial cell number compared to the Ag patches which carry identical Ag deposits. Among the samples of different sputter time (A, 20 s or B, 60 s) the 60 s samples are more effective due to the higher amounts of deposited Ag. Although the co-sputtered Pt/Ag samples seem to exert a higher antimicrobial activity compared to Ag patches alone this effect is not statistically significant.

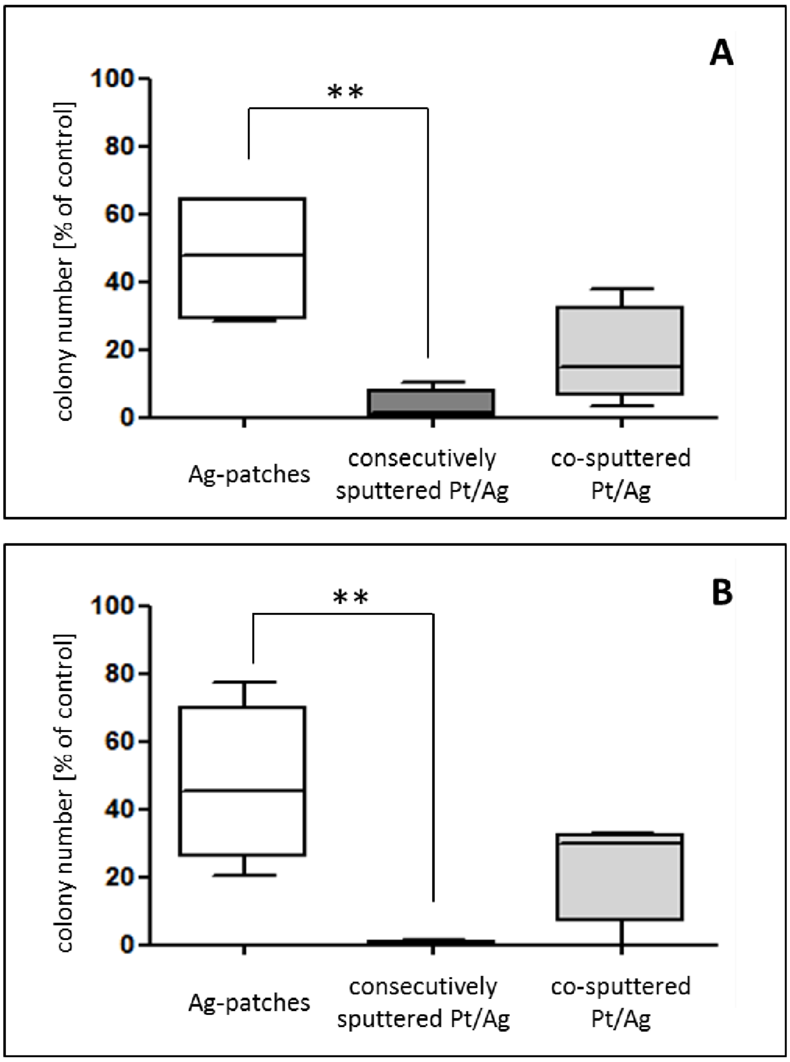

Figure 3. Antibacterial efficiency of different sputtered nanopatches towards *S.aureus*. Bacterial colonies from blood agar plates were counted (drop dilutions of 1 to 10^5). **A**, samples generated with 20 s sputter time; **B**, samples generated with 60 s sputter time. Controls represent Ti samples without sputtered nanopatches. Data are expressed as box-whiskers-plots. Boxes represent 25th - 75th percentile of the data distribution. Median of each group is given as a horizontal line within the boxes, whiskers represent min. and max. values. **, $p< 0.01$, n=4.

To confirm the sacrificial anode effect and to analyze the different antibacterial efficiency of consecutively sputtered samples with the respective co-sputtered samples, electrochemical analyses were performed by voltammetry. As is shown in Figure 4 Ag oxidation peaks are seen for consecutively sputtered Pt/Ag (red line) and co-sputtered samples (green line), but not for the sample with pure Ag nanopatches (black line). The peak starting at about 0.05 V for the consecutively sputtered Pt/Ag sample (red) is attributed to the oxidation of Ag to AgCl.[21, 22]

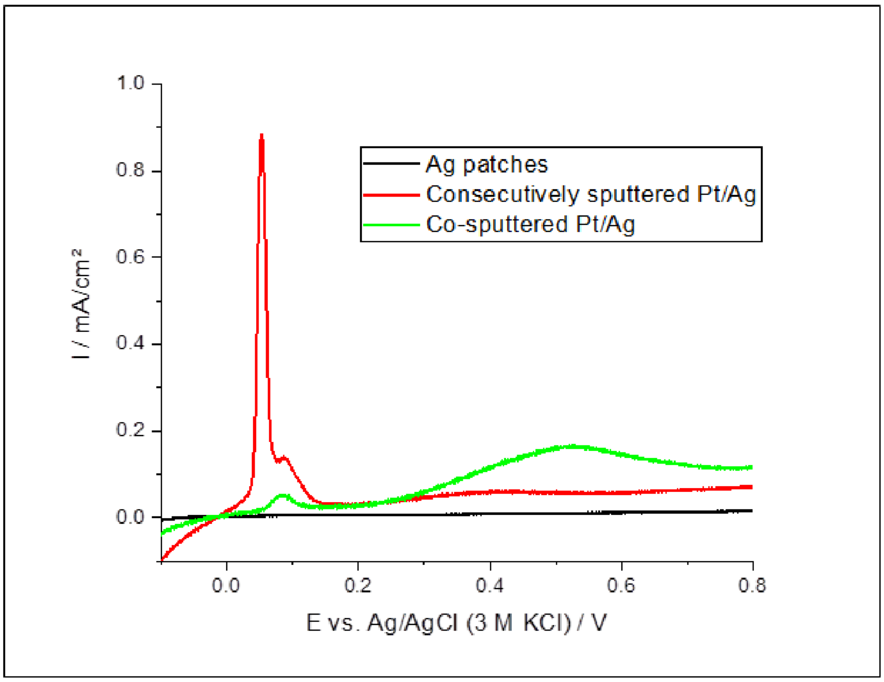

Figure 4. Linear sweep voltammetry (LSV) in 1 M HCl between -0.1 V and 0.8 V at 25 mV/s of an Ag layer 60 s sputtering (black), a Pt layer 60 s sputtering followed by 60 s sputtering of Ag (red) and co-sputtering of Pt and Ag for 60 s (green) on a dense Ti layer.

After the oxidation, the current is almost zero. Thus, quantitative oxidation of the present Ag can be assumed. The co-sputtered sample (green) shows a small (less than 1 mA/cm²) peak attributed the oxidation of Ag to AgCl at ca. 0.1 V. Starting at about 0.25 V, a broad, second oxidation peak is visible stretching over a range of 400 mV. This broad oxidation peak can be associated to the dealloying of a formed AgPt alloy.[23]

The Ag is thermodynamically stabilized by alloying with Pt, therefore it requires higher potentials to oxidize Ag to AgCl.[24] This alloying effect counteracts the wanted sacrificial anode effect and explains the low antibacterial activity of the co-sputtered samples.

The enhanced antimicrobial activity of Pt/Ag nanopatches due to the sacrificial anode effect correlated to an enhanced dissolution of the Ag within a biological environment. This was demonstrated by TEM analysis after immersion of Pt/Ag nanopatches (each 20 s samples) on TEM grids within cell culture medium (RPMI/FCS10%) for 3 d under cell culture conditions (Figure 5).

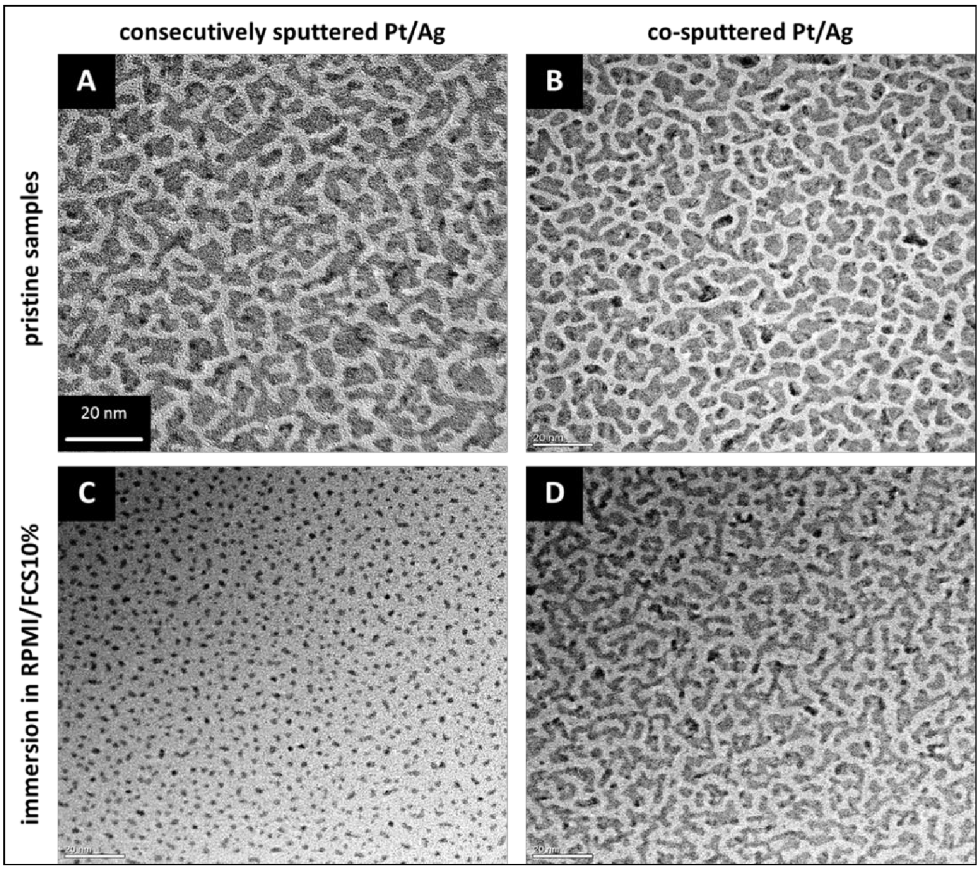

Figure 5. TEM analysis of Pt/Ag nanopatches (sputtered 20 s on TEM grid) after immersion in cell culture medium. Samples were immersed in RPMI/FCS10% for 3 d under cell culture conditions. **A, B** non-immersed (pristine) samples; **C, D** immersed samples. **A, C** consecutively sputtered samples; **B, D** co-sputtered samples. Scale bar 20 nm.

The consecutively sputtered sample (Figure 5 C) revealed dissolution of the Ag compared to the similar but untreated sample (Figure 5 A, pristine sample). The majority of the small remaining deposits are Pt-rich which was confirmed by EDX (data not shown). In contrast, the co-sputtered sample showed only minor Ag dissolution after immersion (Figure 5 D) compared to the non-immersed (pristine) sample (Figure 5 B). The results correlate to the antibacterial and electrochemical analyses and indicate an efficient but time-limited antibacterial effect of consecutively but not co-sputtered Pt/Ag nanopatches.

To analyze the biocompatibility human mesenchymal stem cells (MSC) were seeded onto the highly antibacterial active consecutively sputtered 20s and 60s samples using a similar drop-based method as was used for antibacterial analyses. After an incubation of 24 h under cell culture conditions a significant decrease in biocompatibility was observed (Figure 6, open boxes). However, this decrease in biocompatibility of pristine samples was not observed after a 6h pre-immersion of the samples in pure cell culture medium before cell loading (Figure 6, gray boxes). This indicated the fast dissolution of the Ag patches within the preincubation phase which is self-limited due to the low total Ag amounts of the deposits. During the Ag dissolution period also eukaryotic cells (MSC) were affected. However, after Ag dissolution the adhesion of tissue cells recurred.

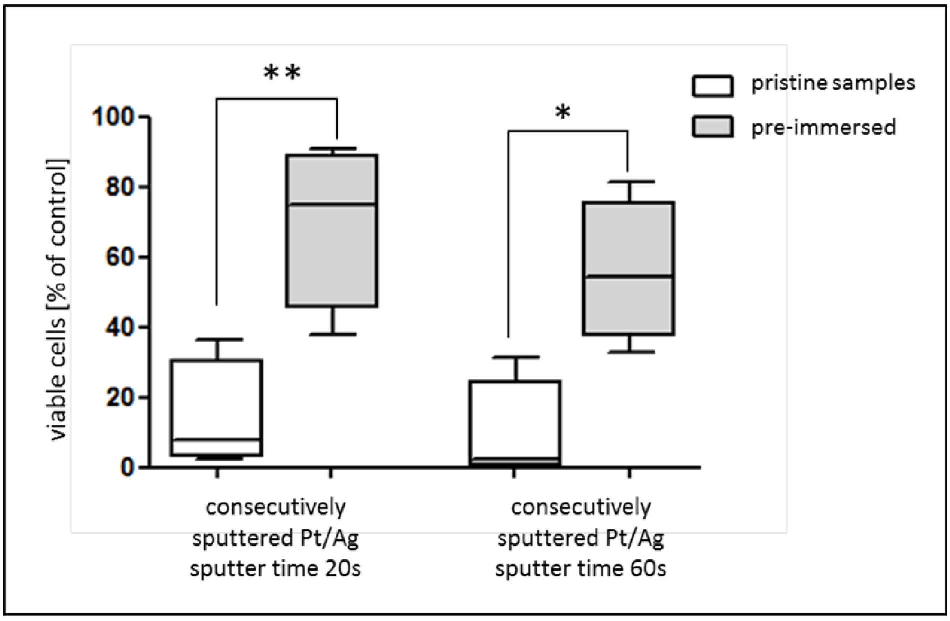

Figure 6. Biocompatibility of different sputtered nanopatches on human mesenchymal stem cells (MSC). Adherent and viable MSC were marked by calcein-AM and quantified by fluorescence microscopy using phase analysis. MSC were incubated on nanopatch samples

(20s and 60s sputter time) for 24 h under cells culture conditions. Open boxes represent pristine samples; grey boxes represent samples which have been pre-incubated in pure cell culture medium and cell culture conditions for 6 h prior to cell loading. Controls represent Ti samples without sputtered nanopatches. Data are expressed as box-whiskers-plots. Boxes represent 25th - 75th percentile of the data distribution. Median of each group is given as a horizontal line within the boxes, whiskers represent min. and max. values. *, p< 0.05 **; p< 0.01, n=4.

.

Discussion

Although there are many studies on Ag for antibacterial biomedical applications, our sacrificial anode approach which leads to enhanced Ag ion release concomitantly to less total Ag amount is unique.[4, 12, 25] In spite of best clinical practice and peri-operative antibiotic treatment remaining prosthetic infections usually originate from contamination during surgery.[26] Once a microbial biofilm has been formed also Ag treatment reaches its limits later on.[27] Therefore, it is of utmost importance to prevent the early adherence and colonization of bacteria to implant surfaces to avoid biofilm formation. For this a high Ag ion releasing capacity of the sacrificial-anode system might be favorable. Significantly, we previously demonstrated that a pure Ag coating did not release sufficient Ag ions to keep an implant surface within an infected tissue-like environment sterile. In contrast to the pure Ag surface, a sacrificial anode sample (Ir/Ag) was able to prevent bacterial growth on the surface under same conditions.[20] The major reason is that the electrochemically induced high release of Ag ions provides sufficient antibacterial activity within the post implantation microenvironment in face of high protein content, limited diffusion or rapid metabolism.[20] Such necessary high silver ion concentrations will always affect also eukaryotic tissue cells in the near vicinity as we have shown previously[. 9, 19] However, the self-limited silver ion release within a short period will allow tissue cells to adhere and to proliferate on the surfaces after silver patch dissolution.

In general, ultra-thin films are increasingly used in nanotechnology for instance for a number of metal-dielectric devices as transmission-induced filters or conductive transparent multilayer structures.[28-30] In contrast to the sputter-deposited Ag/Pt ultrathin nanopatches of this study, Ag/Pt nanoparticles (alloyed-type as well as core/shell-type, 15-25 nm) synthesized by wet-chemistry did not show any sacrificial anode effect for Ag.[23] This effect is obviously due to an increase in the redox potential of Ag in an alloy-like contact to Pt. It was shown by comparable electrochemical analyses that the Ag of alloyed Ag/Au nanoparticles was oxidized at higher potentials.[24] As is shown herein, co-sputtered nanopatches (Pt and Ag at the same time) exhibited also lower antibacterial effects compared to similar nanopatches which were generated by consecutive sputtering. In accordance with our HAADF-STEM results (Figure 1 D-G), we conclude that co-sputtering led to similar thin but more alloy-like deposition (Figure 7 A) whereas a consecutive sputter process led to a kind of layer-on-layer nano-clusters or compositionally inhomogeneous (Figure 7 B) with Pt-rich spherical areas which obviously can act as nano-galvanic elements. In fact, our electrochemical analyses demonstrated an alloy-like response curve in the triggered Ag release from co-sputtered samples compared to similar but consecutively sputtered samples.

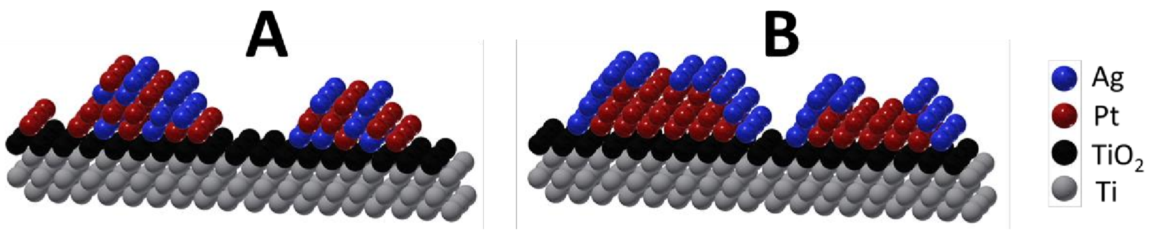

Figure 7. The schemes show the assumed elemental distribution in the nanopatches for co-sputtering which results in an alloy-like deposition **(A)** and consecutive sputtering which leads to layer-on layer nanoclusters **(B).**

It is known that a sacrificial anode effect is influenced by the involved areas of the anode and the related cathode.[31] In this study we focused mainly on approximately equal Ag/Pt areas by use of same sputter time for deposition (20 s and 60 s). However, the presented sacrificial anode system for enhanced Ag release may be further optimized by variations in respective Ag/Pt areas.

In conclusion, we demonstrated the feasibility of a new ultrathin coating using Ag in combination of Pt as nanopatch sputter deposits which benefit in improved antibacterial performance by a sacrificial anode mechanism. These coatings offer some favorable properties such as very low total Ag and Pt amounts, triggered high Ag+ ion release, and the extraordinary thin deposits which topographically follow the primary implant surface. Such implant surfaces may hinder bacterial adhesion at early phases after implantation and allow tissue cell adherence after the phase of silver dissolution.

References

1. Li B, Webster TJ. Bacteria antibiotic resistance: new challenges and opportunities for implant-associated orthopaedic infections. *J Orthop Res* 2018; **36:**22–32.

2. Elbourne A, Crawford RJ, Ivanova EP. Nano-structured antimicrobial surfaces: From nature to synthetic analogues. *J Colloid Interface Sci* 2017; **508:**603-16.

3. Goodman SB, Yao Z, Keeney M, Yang F. The future of biologic coatings for orthopaedic implants. *Biomaterials* 2013; **34:**3174-83.

4. Alt V. Antimicrobial coated implants in trauma and orthopaedics-A clinical review and risk-benefit analysis. *Injury* 2017; **48**:599-607.

5. Chernousova S, Epple M. Silver as antibacterial agent. Ion, nanoparticle, and metal. *Angew. Chem. Int. Ed. Engl.* 2013; **52**:1636-53.

6. Cameron SJ, Hosseinian F, Willmore WG. A current overview of the biological and cellular effects of nanosilver. *Mol Sci* 2018; **19**: 2030.

7. Loza K, Diendorf J, Greulich C, Ruiz-Gonzalez L, Gonzalez-Calbet J, Vallet-Regi, et al. The dissolution and biological effects of silver nanoparticles in biological media. *J Mater Chem B* 2014; **2:**1634-43.

8. Liu JY, Hurt RH. Ion release kinetics and particle persistence in aqueous nano-silver colloids. *Environ Sci Technol* 2010; **44**: 2169-75.

9. Loza K, Sengstock C, Chernousova S, Köller M, Epple M. The predominant species of ionic silver in biological media is colloidally dispersed nanoparticulate silver chloride. *RSC Adv* 2014; **4**:35290.

10. Kaiser JP, Roesslein M, Diener L, Wichser A, Nowack B, Wick P. Cytotoxic effects of nanosilver are highly dependent on the chloride concentration and the presence of organic compounds in the cell culture media. *J Nanobiotechnol* 2017; **15**:5.

11. Lansdown AGB. A pharmacological and toxicological profile of silver as an antimicrobial agent in medical devices. *Adv Pharmacol Sci* 2010; **2010:**910686.

12. Akter M, Sikder MT, Rahman MM, Ullah AKMA, Hossain KFB, Banik S, et al. A systematic review on silver nanoparticles-induced cytotoxicity: Physicochemical properties and perspectives. *J Adv Res* 2018; **9**:1-16.

13. Ullah Khan S, Saleh TA, Wahab A, Khan MHU, Khan D, Ullah Khan W, et al. Nanosilver: new ageless and versatile biomedical therapeutic scaffold. *Int J Nanomed* 2018; **12:**733–62.

14. Reidy B, Haase A, Luch A, Dawson KA, Lynch I. Mechanisms of silver nanoparticle release, transformation and toxicity: a critical review of current knowledge and recommendations for future studies and applications, *Materials* 2013; **6:** 2295-350.

15. M. Köller, C. Sengstock, Y. Motemani, C. Khare, P.J. Buenconsejo, J. Geukes, et al. Antibacterial activity of microstructured Ag/Au sacrificial anode thin films. *Mater Sci Eng C* 2015; **46**:276-80.

16. Köller M, Bellova P, Javid SM, Motemani Y, Khare C, Sengstock C, et al. Antibacterial activity of microstructured sacrificial anode thin films by combination of silver with platinum group elements (platinum, palladium, iridium). *Mater Sci Eng C* 2017; **74:**536-41.

17. Szabo S, Bakos I. Cathodic protection with sacrificial anodes. *Corros Rev* 2006; **24:**231-80.

18. El Arrassi A, Bellova P, Javid SM, Motemani Y, Khare C, Sengstock C, et al. A unified interdisciplinary approach to design antibacterial coatings for fast silver release. *Chem Electro Chem* 2017; **4:**1975-83.

19. Greulich C, Braun D, Peetsch A, Diendorf J, Siebers B, Epple M, et al. The toxic effect of silver ions and silver nanoparticles towards bacteria and human cells occurs in the same concentration range. *RSC Advances* 2012; **2:**6981–7.

20. Abuayyash A, Ziegler N, Gessmann J, Sengstock C, Schildhauer TA, Ludwig A, et al. Antibacterial efficacy of sacrifical anode thin films combining silver with platinum group elements within a bacteria-containing human plasma clot. *Adv Eng Mater* 2017; 1700493.

21. Saw EN, Kratz M, Tschulik K. Time-resolved impact electrochemistry for quantitative measurement of single-nanoparticle reaction kinetics. Nano Res 2017; **10:**3680–9.

22. Saw EN, Blanc N, Kanokkanchana K, Tschulik K. Time-resolved impact electrochemistry – A new method to determine diffusion coefficients of ions in solution. *Electrochimica Acta* 2018; **282:**317-23.

23. Grasmik V, Rurainsky C, Loza K, Evers MV, Prymak O, Heggen M, et al. Deciphering the surface composition and the internal structure of alloyed silver-gold nanoparticles. *Chemistry 2018*; **24**:9051-60.

24. Saw EN, Grasmik V, Rurainsky C, Epple M, Tschulik K. Electrochemistry at single bimetallic nanoparticles - using nano impacts for sizing and compositional analysis of individual AgAu alloy nanoparticles. *Faraday Discuss* 2016; **193:**327-38.

25. Kuehl R, Brunetto PS, Woischnig AK, Varisco M, Rajacic Z, Vosbeck J, et al. Preventing implant-associated infections by silver coating. *Antimicrob Agents Chemother* 2016; **60**: 2467-75.

26. Arciola CR, Carla R, Campoccia D, Montanaro L. Implant infections: adhesion, biofilm formation and immune evasion. *Nat Rev Microbio* 2018; **16:**397-409.

27. Fennell Y, Ymele-Leki P, Azeezat Adegboye T, Jones K. Impact of sulfidation of silver nanoparticles on established P. aeruginosa biofilm. *J Biomat Nanobiotech* 2017; **8:**83-95.

28. Bulir J, Novotny M, Lynnykova A, Lancok J. Preparation of nanostructured ultrathin silver layer. *J Nanophotonics* 2011; **5**:051511.

29. Winkler T, Schmidt H, Flügge H, Nikolayzik F, Baumann I, Schmale S, et al. Realization of ultrathin silver layers in highly conductive and transparent zinc tin oxide/silver/zinc tin oxide multilayer electrodes deposited at room temperature for transparent organic devices. *Thin Solid Films* 2012; **520:**4669-73.

30. Devaraj V, Lee J, Baek J, Lee D. Fabrication of ultra-smooth 10 nm silver films without wetting layer. *Appl Sci Converg Technol* 2016; **25:**32-5.

31. Zhang XG, Galvanic Corrosion: In Revie RW, editor. *Uhlig's Corrosion Handbook*. 3rd ed. Hoboken: Wiley & Sons; 2011, p. 123–44.